

# Ketones and lactate “fuel” tumor growth and metastasis

## Evidence that epithelial cancer cells use oxidative mitochondrial metabolism

Gloria Bonuccelli,<sup>1,2</sup> Aristotelis Tsirigos,<sup>3</sup> Diana Whitaker-Menezes,<sup>1,2</sup> Stephanos Pavlides,<sup>1,2</sup> Richard G. Pestell,<sup>1,2</sup> Barbara Chiavarina,<sup>1,2</sup> Philippe G. Frank,<sup>1,2</sup> Neal Flomenberg,<sup>4</sup> Anthony Howell,<sup>5</sup> Ubaldo E. Martinez-Outschoorn,<sup>1,2,4</sup> Federica Sotgia<sup>1,2,5\*</sup> and Michael P. Lisanti<sup>1,2,4,5\*</sup>

<sup>1</sup>Departments of Stem Cell Biology & Regenerative Medicine, Cancer Biology; and <sup>4</sup>Medical Oncology; <sup>2</sup>The Jefferson Stem Cell Biology and Regenerative Medicine Center; Kimmel Cancer Center; Thomas Jefferson University; Philadelphia, PA USA; <sup>3</sup>Computational Genomics Group, IBM Thomas J. Watson Research Center; Yorktown Heights, NY USA; <sup>5</sup>Manchester Breast Centre & Breakthrough Breast Cancer Research Unit; Paterson Institute for Cancer Research; School of Cancer, Enabling Sciences and Technology; Manchester Academic Health Science Centre; University of Manchester; UK

**Key words:** 3-hydroxybutyrate (ketone bodies), L-lactate, stroma, tumor growth, metastasis, the Warburg effect, aerobic glycolysis, tumor microenvironment, cancer associated fibroblasts

Previously, we proposed a new model for understanding the “Warburg effect” in tumor metabolism. In this scheme, cancer-associated fibroblasts undergo aerobic glycolysis and the resulting energy-rich metabolites are then transferred to epithelial cancer cells, where they enter the TCA cycle, resulting in high ATP production via oxidative phosphorylation. We have termed this new paradigm “The Reverse Warburg Effect.” Here, we directly evaluate whether the end-products of aerobic glycolysis (3-hydroxy-butyrates and L-lactate) can stimulate tumor growth and metastasis, using MDA-MB-231 breast cancer xenografts as a model system. More specifically, we show that administration of 3-hydroxy-butyrates (a ketone body) increases tumor growth by ~2.5-fold, without any measurable increases in tumor vascularization/angiogenesis. Both 3-hydroxy-butyrates and L-lactate functioned as chemo-attractants, stimulating the migration of epithelial cancer cells. Although L-lactate did not increase primary tumor growth, it stimulated the formation of lung metastases by ~10-fold. Thus, we conclude that ketones and lactate fuel tumor growth and metastasis, providing functional evidence to support the “reverse Warburg effect.” Moreover, we discuss the possibility that it may be unwise to use lactate-containing i.v. solutions (such as lactated Ringer’s or Hartmann’s solution) in cancer patients, given the dramatic metastasis-promoting properties of L-lactate. Also, we provide evidence for the upregulation of oxidative mitochondrial metabolism and the TCA cycle in human breast cancer cells *in vivo*, via an informatics analysis of the existing raw transcriptional profiles of epithelial breast cancer cells and adjacent stromal cells. Lastly, our findings may explain why diabetic patients have an increased incidence of cancer, due to increased ketone production, and a tendency towards autophagy/mitophagy in their adipose tissue.

### Introduction

Previously, we identified a loss of stromal caveolin-1 (Cav-1), in the cancer-associated fibroblast compartment, as a single independent predictor of early tumor recurrence, lymph node metastasis, tamoxifen-resistance and poor clinical outcome, in human breast cancer patients.<sup>1</sup> Importantly, these findings were independent of epithelial marker status, indicating that the prognostic value of a loss of stromal Cav-1 applies to all of the most common sub-types of invasive ductal carcinoma.<sup>1</sup> These findings have now been validated in three different cohorts of human breast cancer patients, including a cohort of triple negative and basal-like breast cancer

patients.<sup>1-3</sup> In triple negative patients, high expression of stromal Cav-1 was associated with a survival rate of 75.5% at 12 years post-diagnosis.<sup>2</sup> Conversely, an absence of stromal Cav-1 in the same triple negative patient population was associated with a survival rate of less than 10% at five years post-diagnosis.<sup>2</sup> Thus, it is imperative that we mechanistically understand the prognostic value of stromal Cav-1, as it could lead to new therapeutic strategies for the treatment of human breast cancers and other types of cancer. In further support of this notion, a loss of stromal Cav-1 in DCIS patients is associated with a 100% rate of lesion recurrence and 80% of these patients progressed to invasive breast cancer.<sup>4</sup> Finally, a loss of stromal Cav-1 in prostate cancer patients was strictly associated

\*Correspondence to: Michael P. Lisanti; Email: michael.lisanti@kimmelcancercenter.org and Federica Sotgia; Email: federica.sotgia@jefferson.edu

Submitted: 06/18/10; Accepted: 06/21/10

Previously published online: [www.landesbioscience.com/journals/cc/article/12731](http://www.landesbioscience.com/journals/cc/article/12731)

DOI: 10.4161/cc.9.17.12731

with advanced prostate cancer and metastatic disease progression, as well as high Gleason score—indicative of a poor prognosis.<sup>5</sup>

To understand the prognostic value of a loss of stromal Cav-1, we next turned to Cav-1(-/-) null mice as a model experimental system.<sup>6</sup> From these mice, we isolated bone marrow stromal cells, which are thought to be the precursors of cancer associated fibroblasts and subjected them to unbiased proteomics analysis, as well as genome-wide transcriptional profiling.<sup>7</sup> Using this proteomics approach, we demonstrated that Cav-1 (-/-) null stromal cells show the overexpression of three major classes of proteins: (1) eight myofibroblast markers (such as vimentin, calponin and collagen I); (2) eight glycolytic enzymes (including PKM2 and LDHA); and (3) two anti-oxidants (namely, catalase and peroxiredoxin).<sup>7</sup> Virtually identical results were obtained by genome-wide transcriptional profiling, directly implicating the activation of HIF and NFκB, as key transcription factors during a loss of Cav-1 in stromal cells.<sup>8</sup> Furthermore, the upregulation of glycolytic enzymes under normoxic conditions is consistent with the onset of the Warburg effect, a.k.a, aerobic glycolysis. However, the “classical” Warburg effect was thought to be largely confined to cancer epithelial cells, and has never been extended to the cancer associated fibroblast compartment. Induction of glycolysis under conditions of normoxia can be accomplished via oxidative stress, possibly explaining the overexpression of anti-oxidant enzymes in Cav-1 (-/-) deficient stromal cells.<sup>8</sup> Importantly, we validated the selective expression of glycolytic enzymes (PKM2 and LDHA/B/C) in the fibroblastic stroma of human breast cancer patients that lack stromal Cav-1 expression.<sup>7,9</sup>

Based on these and other supporting findings, we proposed a new model for understanding the Warburg effect in tumor metabolism.<sup>7,10</sup> In this model, epithelial cancer cells induce aerobic glycolysis in adjacent cancer-associated fibroblasts, directing them to produce energy-rich metabolites (such as lactate and 3-hydroxy-butyrate).<sup>7,10</sup> Then, these metabolites would be transferred to the epithelial cancer cells, where they can then enter the mitochondrial TCA cycle, undergo oxidative phosphorylation, resulting high ATP production.<sup>7,10</sup> We have termed this new model “the reverse Warburg effect.”<sup>7,10</sup>

In direct support of these findings, we have recently shown using a co-culture model, that MCF7 epithelial cancer cells have the ability to downregulate both Cav-1 expression and mitochondria in adjacent fibroblasts via the induction of autophagy/mitophagy.<sup>11,12</sup> This then drives aerobic glycolysis in the fibroblast compartment.<sup>11,12</sup> More specifically, MCF7 cells induce oxidative stress in adjacent fibroblasts.<sup>11</sup> Oxidative stress is then sufficient to drive the induction of autophagy/mitophagy in fibroblasts, leading to Cav-1 lysosomal degradation and aerobic glycolysis.<sup>11</sup> Conversely, during co-culture, we observed that MCF7 epithelial cancer cells dramatically increase their mitochondrial mass and mitochondrial activity.<sup>11</sup> Moreover, we could phenocopy these effects by simply adding L-lactate (an end product of glycolysis) to the tissue culture media of MCF7 cells.<sup>11</sup> Under these conditions, L-lactate treatment was sufficient to dramatically increase mitochondrial mass in MCF7 cancer cells.<sup>11</sup>

Based on the above biomarker and mechanistic experiments, we have proposed that the Cav-1 (-/-) mammary fat pad can be

used as a pre-clinical model of a “lethal” tumor microenvironment.<sup>8</sup> With this in mind, we subjected Cav-1 (-/-) null mammary fat pads to an unbiased metabolomics analysis.<sup>13</sup> The results obtained provided independent validation for the idea that a loss of stromal Cav-1 induces oxidative stress, which in turn activates autophagy/mitophagy, leading to aerobic glycolysis.<sup>13</sup> Importantly, 3-hydroxy-butyrate (a ketone body) is one of the key metabolites that was most significantly elevated, over four-fold.<sup>13</sup> 3-Hydroxy-butyrate is another metabolic end-product of glycolysis (which can be derived from pyruvate)<sup>13</sup> that accumulates during starvation and mitochondrial dysfunction, and is elevated in diabetic patients.

There are several important parallels between 3-hydroxy-butyrate and L-lactate. Both can be considered metabolic end-products of glycolysis, derived from pyruvate. 3-hydroxy-butyrate and L-lactate are both secreted and take up by the same monocarboxylate transporters (MCTs). After uptake by MCTs, they can both re-enter the TCA cycle as acetyl-CoA and undergo oxidative metabolism, resulting in the production of high levels of ATP. Thus, based on these findings, we have proposed that both ketones and lactate (produced via aerobic glycolysis in fibroblasts) could fuel tumor growth and metastasis in epithelial cancer cells.<sup>13</sup> However, this hypothesis remains to be tested experimentally.

Here, we have employed a xenograft model of human breast cancer to assess the possible tumor promoting properties of the end-products of aerobic glycolysis, namely ketones and lactate. For this purpose, we chose MDA-MB-231 human breast cancer cells, which show a marker profile most consistent with triple negative and basal-like breast cancers. MDA-MB-231 cells were grown in athymic nude mice as solid tumors via flank injections, or were induced to undergo lung metastasis via tail vein injections. Then, we systemically administered 3-hydroxy-butyrate or L-lactate via intra-peritoneal (i.p.) injections. Our results clearly show that 3-hydroxy-butyrate or L-lactate “fuel” tumor growth and metastasis, without a measurable increase in tumor angiogenesis. Thus, our results provide metabolic/functional evidence to directly support the “reverse Warburg effect.” Via an informatics analysis of the existing raw transcriptional profiles of epithelial cancer cells and adjacent stromal cells,<sup>14</sup> we also provide evidence for the upregulation of oxidative phosphorylation, the TCA cycle and mitochondrial metabolism in human breast cancer cells *in vivo*.

## Results

**Ketones promote tumor growth, without any increase in angiogenesis.** To evaluate the potential tumor-promoting properties of the products of aerobic glycolysis (such as 3-hydroxy-butyrate and L-lactate), we used a xenograft model employing MDA-MB-231 breast cancer cells injected into the flanks of athymic nude mice. Tumor growth was assessed by measuring tumor volume, at three weeks post-tumor cell injection. During this time period, mice were administered either PBS alone or PBS containing 3-hydroxy-butyrate (500 mg/kg) or L-lactate (500 mg/kg), via daily intra-peritoneal (i.p.) injections.

Interestingly, **Figure 1** shows that 3-hydroxy-butyrate is sufficient to promote an ~2.5-fold increase in tumor growth, relative to the PBS-alone control. Under these conditions, L-lactate had no significant effect on tumor growth.

One mechanism that could account for the tumor-promoting properties of 3-hydroxy-butyrate is increased tumor angiogenesis. Thus, we evaluated the status of tumor vascularity using antibodies directed against CD31. Interestingly, **Figure 2** shows that the vascular density (number of vessels per field) was not increased by the administration of either 3-hydroxy-butyrate or L-lactate. Thus, other mechanisms, such as the “reverse Warburg effect” may be operating to increase tumor growth.

**Ketones and lactate function as chemo-attractants, stimulating cancer cell migration.** Next, we assessed whether 3-hydroxy-butyrate or L-lactate can function as chemo-attractants, using a modified “Boyden Chamber” assay, employing Transwell cell culture inserts. MDA-MB-231 cells were placed in the upper chambers and 3-hydroxy-butyrate (10 mM) or L-lactate (10 mM) were introduced into the lower chambers. Interestingly, using this assay system, both 3-hydroxy-butyrate and L-lactate promoted cancer cell migration by nearly 2-fold (**Fig. 3**). Thus, the metabolic products of aerobic glycolysis can also function as chemo-attractants for cancer cells, probably via a form of nutrient sensing.

**Lactate fuels lung metastasis.** Finally, we tested the effect of 3-hydroxy-butyrate and L-lactate on cancer cell metastasis. For this purpose, we used a well-established lung colonization assay, where MDA-MB-231 cells are injected into the tail vein of athymic nude mice. After 7 weeks post-injection, the lungs were harvested and the metastases were visualized with India ink staining. In this method, the lung parenchyma stains black, while the tumor metastatic foci remain unstained and appear white. For quantitation purposes, the number of metastases per lung lobe was scored.

**Figure 4A** shows that relative to PBS-alone, the administration of L-lactate stimulated the formation of metastatic foci by ~10-fold. Under these conditions, 3-hydroxy-butyrate had no effect on metastasis formation. Representative examples of lung metastasis in PBS-alone controls and L-lactate-treated animals are shown in **Figure 4B**. Note that the metastatic foci formed in L-lactate treated animals are more numerous, and are also larger in size.

Thus, 3-hydroxy-butyrate fuels tumor growth, while L-lactate stimulates lung metastasis. As such, the “tumor-promoting” effects of 3-hydroxy-butyrate and L-lactate are remarkably specific to a given phase of tumor progression.

**Human breast cancer epithelial cells in vivo show the induction of mitochondrial oxidative phosphorylation, relative to adjacent tumor stromal cells.** To further validate the model that human breast cancer cells show a shift towards mitochondrial oxidative metabolism, we re-interrogated raw transcriptional profiling

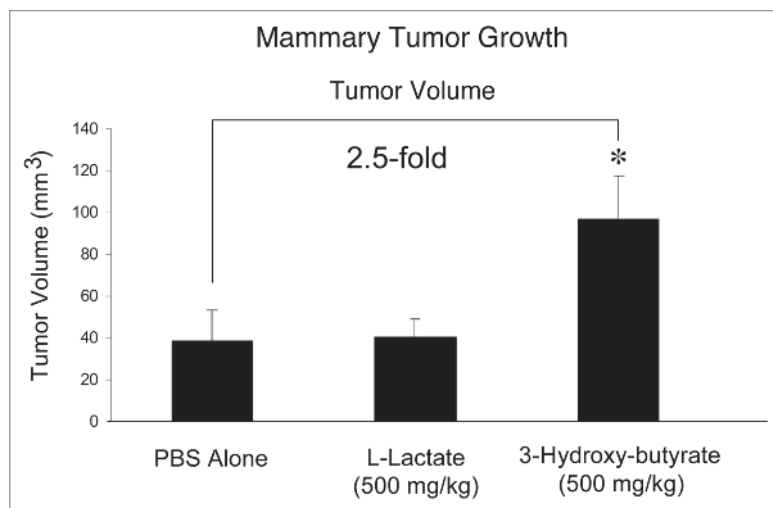


**Figure 1.** Ketones promote tumor growth. We used a xenograft model employing MDA-MB-231 breast cancer cells injected into the flanks of athymic nude mice to evaluate the potential tumor promoting properties of the products of aerobic glycolysis (such as 3-hydroxy-butyrate and L-lactate). Tumor growth was assessed by measuring tumor volume, at 3-weeks post tumor cell injection. During this time period, mice were administered either PBS alone or PBS containing 3-hydroxy-butyrate (500 mg/kg) or L-lactate (500 mg/kg), via daily intra-peritoneal (i.p.) injections. Note that 3-hydroxy-butyrate is sufficient to promote an ~2.5-fold increase in tumor growth, relative to the PBS-alone control. Under these conditions, L-lactate had no significant effect on tumor growth. \* $p < 0.05$ , PBS alone versus 3-hydroxy-butyrate (Student's t-test).  $N = 8$  tumors for the PBS group.  $N = 10$  tumors each, for L lactate and 3-Hydroxy-butyrate groups

data obtained by laser-capture micro-dissection of human breast cancer samples. In this data set, breast cancer epithelial cells and adjacent tumor stroma were isolated from the same tumors,<sup>14</sup> allowing their direct comparison by transcriptional profiling.

For this purpose, we generated a list of genes that were transcriptionally upregulated in human breast cancer epithelial cells, relative to the adjacent stromal cells (**Suppl. Table 1**). Then, this list of genes was intersected with existing databases to determine the cellular processes that were upregulated in epithelial cancer cells, relative to adjacent stromal cells. Interestingly, using this approach, we see that numerous gene sets associated with oxidative mitochondrial metabolism are indeed increased or “enriched” in human breast cancer cells, relative to adjacent stromal cells (**Table 1**). Conversely, this means that oxidative mitochondrial metabolism is downregulated in the tumor stromal compartment, relative to the cancer cells, consistent with the “reverse Warburg effect.”

Moreover, the genes that were upregulated in epithelial cancer cells were also downregulated in response to starvation, hypoxia and Alzheimer disease/aging (associated with oxidative stress) (**Table 1**). This is a strong indication that these epithelial cancer cells are not experiencing starvation, hypoxia or oxidative stress, as they are presumably being “fed” by glycolysis in adjacent stromal cells.

Interestingly, the number one gene upregulated in cancer cells, relative to stromal cells, is a subunit of the mitochondrial enzyme isocitrate dehydrogenase (IDH3B; ~7.5-fold increased;

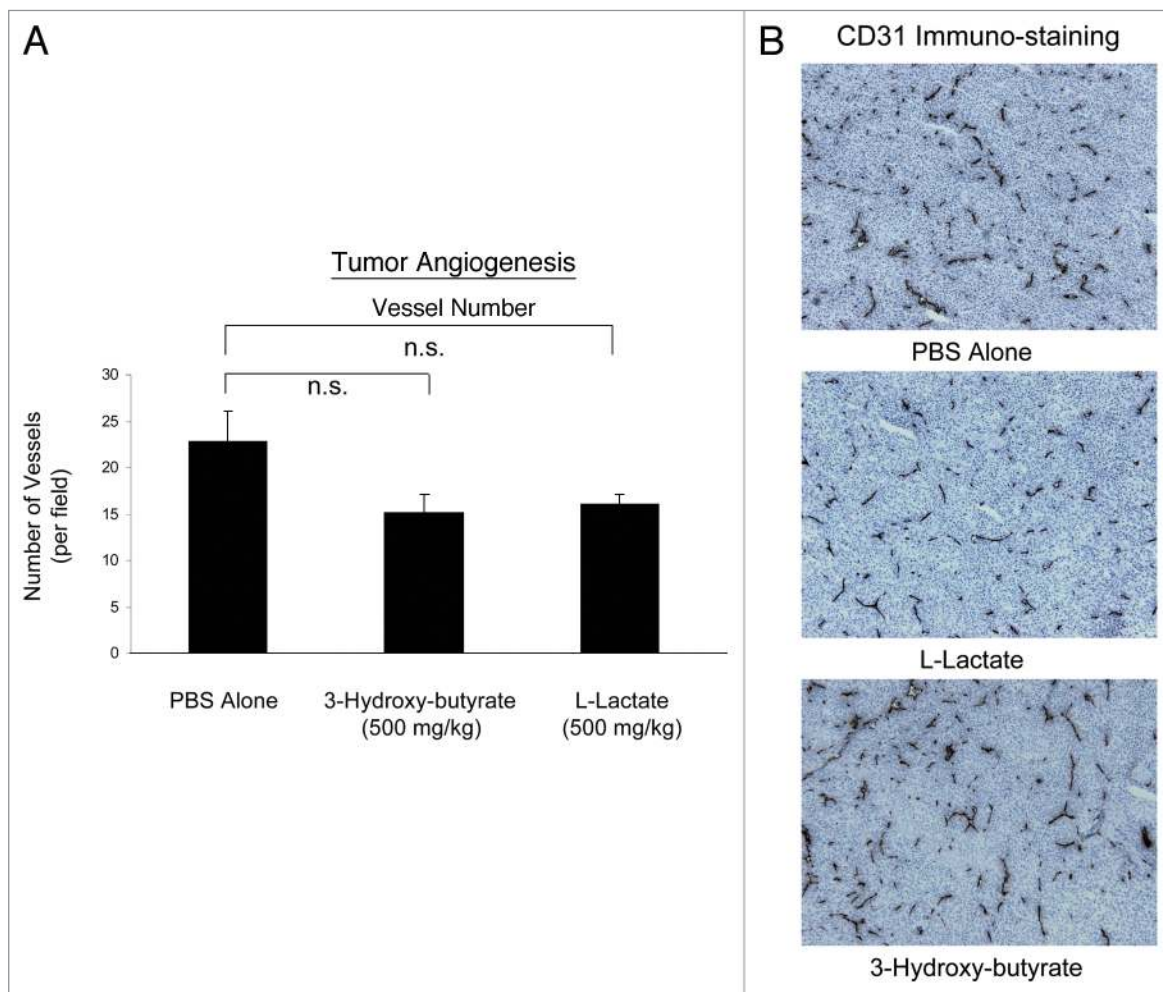


**Figure 2.** Ketones promote tumor growth without any increase in angiogenesis. Tumor angiogenesis could account for the tumor-promoting properties of 3-hydroxy-butyrate. Thus, we next evaluated the status of tumor vascularity using antibodies directed against CD31. However, the vascular density (number of vessels per field) was not increased by the administration of either 3-hydroxy-butyrate or L-lactate. Thus, other mechanisms, such as the “reverse Warburg effect” may be operating to increase tumor growth. (A) Quantitation; (B) Representative images of CD31 immuno-staining in primary tumor samples. n.s., not significant.

$p = 3.2 \times 10^{-10}$ ) which catalyzes the oxidative de-carboxylation of isocitrate to 2-oxoglutarate, in the TCA cycle (Suppl. Table 1). During hypoxia, 2-oxoglutarate would accumulate, leading to HIF-stabilization via inhibition of the prolyl-hydroxylases. However, this appears not to be the case in the epithelial cancer cells, as the genes that cancer cells upregulate are downregulated in response to hypoxia and/or HIF1 $\alpha$  activation (Table 1). This is a further indication that the epithelial cancer cells are indeed using oxidative mitochondrial metabolism.

These results provide independent clinically-relevant evidence that human epithelial breast cancer cells in vivo use oxidative mitochondrial metabolism in patients.

## Discussion

Here, we provide the first evidence that the end-products of aerobic glycolysis (namely, 3-hydroxy-butyrate and L-lactate) can fuel tumor growth and metastasis, when administered systemically in

a human tumor xenograft model. More specifically, we show that 3-hydroxy-butyrate is sufficient to promote a 2.5-fold increase in tumor volume, without any significant increase in angiogenesis. Although L-lactate did not increase tumor growth, it had a significant effect on lung colonization/metastasis, resulting in a 10-fold increase in the formation of metastatic tumor foci. Our results are consistent with the idea that human breast cancer cells can re-utilize the energy-rich end-products of glycolysis for oxidative mitochondrial metabolism. Consistent with these functional xenograft data, we also show, using a transcriptional informatics analysis, that oxidative mitochondrial metabolism is indeed upregulated in human breast cancer cells, relative to adjacent stromal tissue.

**Ketones and tumor growth: The diabetes-cancer connection.** Ketones are a “super-fuel” for mitochondria, producing more energy than lactate and simultaneously decreasing oxygen consumption.<sup>15-17</sup> In fact, because of these properties, ketones have been used to prevent ischemic tissue damage, in animal models undergoing either myocardial infarctions or stroke,



leading to dramatically smaller ischemic/necrotic lesion area.<sup>18,19</sup> So, just as ketones are a “super-fuel” under conditions of ischemia in the heart and in the brain, they could fulfill a similar function during tumorigenesis, as the hypoxic tumor exceeds its blood supply. Stromal ketone production could obviate the need for tumor angiogenesis. Once ketones are produced and released from stromal cells, they could then be re-utilized by epithelial cancer cells, where they could directly enter the TCA cycle, just like lactate. In this sense, ketones are a more powerful mitochondrial fuel, as compared with lactate.

Thus, our current observations may also explain the close and emerging association between diabetes and cancer susceptibility.<sup>20</sup> A number of elegant studies have been carried out in mouse animal models to assess this association and chemical induction of diabetes in rats with streptozocin is sufficient to enhance tumor growth.<sup>21</sup> Similarly, acute fasting in rodent animal models is also sufficient to dramatically increase tumor growth.<sup>22</sup> Both of these experimental conditions (diabetes and fasting/starvation) are known to be highly ketogenic and, thus, are consistent with our current hypothesis that ketone production fuels tumor growth. Finally, given our current findings that ketones increase tumor growth, cancer patients and their dieticians may want to re-consider the use of a “ketogenic diet” as a form of anti-cancer therapy.

**Lactate drives metastatic disease progression: Quercetin and lactated Ringer’s solution.** Tumor lactate production, serum lactate levels and serum LDH levels have long been known as biomarkers for poor clinical outcome in many different types of human epithelial cancers, including breast cancer.<sup>23–33</sup> In fact, lactic-acidosis (due to the over-production and/or accumulation of serum lactate) is often the cause of death in patients with metastatic breast cancer, or other types of metastatic cancer.<sup>34–49</sup> However, a causative role for L-lactate production in tumor metastatic progression has not yet been suggested or demonstrated.

Here, we have directly demonstrated that L-lactate can play a causative role in breast cancer cell metastasis, by increasing the number of lung metastatic foci by ~10-fold. This provides the necessary evidence that mitochondrial oxidative metabolism can also fuel cancer cell metastasis. This may have important clinical implications, as MCT/lactate transport inhibitors could be used therapeutically to suppress tumor metastasis. Our findings could also explain the multiple therapeutic activities of quercetin. Quercetin is a naturally occurring dietary flavenoid (available as an over-the-counter supplement) that functions both as an MCT/lactate transport inhibitor and inhibitor of TGFβ signaling.<sup>50–52</sup> One explanation for these dual activities is that L-lactate uptake into tumor cells somehow metabolically activates TGFβ signaling. As such, the inhibitory effects of quercetin on TGFβ signaling may be due to its ability to inhibit the uptake of L-lactate into tumor cells, presumably resulting in reduced cell migration and metastasis. Further studies will be necessary to address this attractive possibility.

Finally, given the pro-metastatic activity of L-lactate, its medical use in cancer patients should be restricted. However, nearly every oncology surgeon worldwide uses “lactated Ringer’s” (which contains 28 mM L-lactate) as an intravenous (i.v.) solution in cancer patients, before, during and after tumor excision and

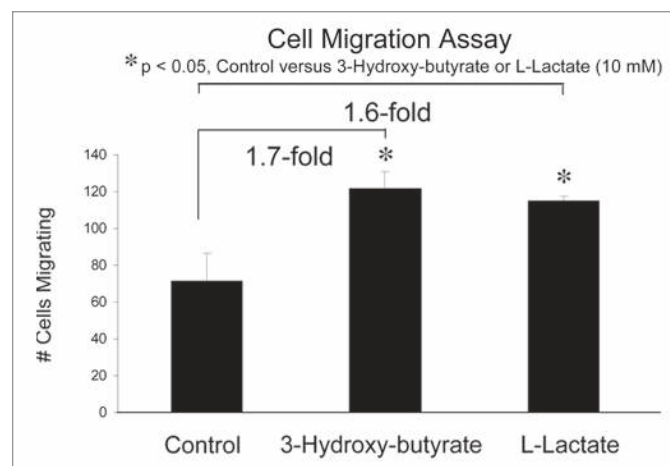


**Figure 3.** Ketones and lactate function as chemo-attractants, stimulating cancer cell migration. We assessed whether 3-hydroxy-butyrate or L-lactate can function as chemo-attractants, using a modified “Boyden Chamber” assay, employing Transwell cell culture inserts. MDA-MB-231 cells were placed in the upper chambers and 3-hydroxy-butyrate (10 mM) or L-lactate (10 mM) were introduced into the lower chambers. Note that both 3-hydroxy-butyrate and L-lactate promoted cancer cell migration by nearly 2-fold. \* $p < 0.05$ , control (vehicle alone) versus 3-hydroxy-butyrate or L-lactate (10mM) (Student’s t-test).

possibly during the entire extended post-operative hospital stay. Based on our current studies, the use of “lactated Ringer’s” in cancer patients may unnecessarily increase their risk for progression to metastatic disease. Thus, oncology surgeons may wish to re-consider using “lactated Ringer’s” solution in cancer patients.

## Materials and Methods

**Materials.** Antibodies for immuno-staining were obtained from commercial sources: CD31 (cat# 550274, BD Biosciences, Inc.). Sodium L-lactate and the ketone 3-Hydroxybutyric acid, sodium salt (3-hydroxy-butyrate) were purchased from Sigma-Aldrich. MDA-MB-231 (GFP<sup>+</sup>) cells were the generous gift of Dr. A. Fatatis (Drexel University, Philadelphia, PA). Migration assays were performed using modified non-coated Boyden chambers (cat#354578) (Transwells; BD Biosciences, San Jose, CA). The Streptavidin-HRP kit was from Dako (Carpinteria, CA).

**Animal studies.** All animals were housed and maintained in a pathogen-free environment/barrier facility at the Kimmel Cancer Center at Thomas Jefferson University under National Institutes of Health (NIH) guidelines. Mice were kept on a 12-hour light/dark cycle with ad libitum access to chow and water. Approval for all animal protocols used for this study was review and approved by the Institutional Animal Care and Use Committee (IACUC). For primary tumor formation, tumor cells [MDA-MB-231 (GFP<sup>+</sup>) ( $1 \times 10^6$  cells)] were re-suspended in 100  $\mu$ l of sterile PBS and injected into the flanks of athymic NCR nude mice (NCRNU; Taconic Farms; 6–8 weeks of age). At 3 weeks post-injection, mice were sacrificed and the tumors were carefully excised and sized using calipers. The formula  $(X^2Y)/2$ ,

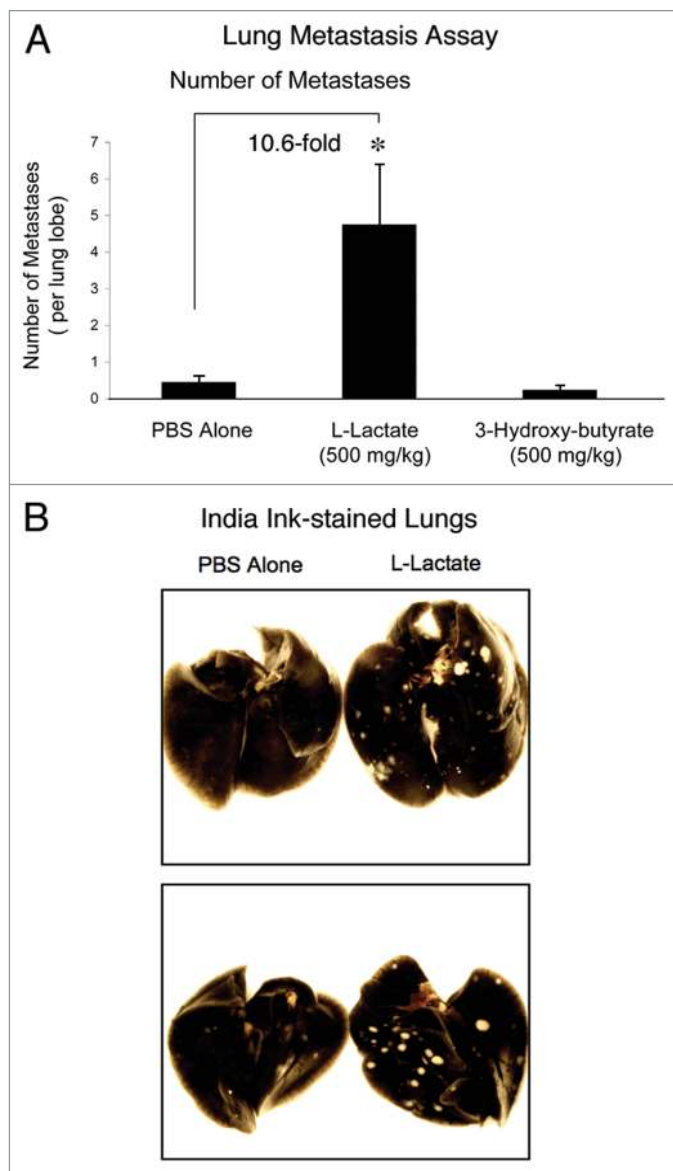


**Figure 4.** Lactate fuels lung metastasis. To examine the effect of 3-hydroxy-butyrate and L-lactate on cancer cell metastasis, we used a well-established lung colonization assay, where MDA-MB-231 cells are injected into the tail vein of athymic nude mice. After 7 weeks post-injection, the lungs were harvested and the metastases were visualized with India ink staining. Using this approach, the lung parenchyma stains black, while the tumor metastatic foci remain unstained and appear white. (A) Quantitation. The number of metastases per lung lobe was scored. Note that relative to PBS-alone, the administration of L-lactate stimulated the formation of metastatic foci by ~10-fold. Under these conditions, 3-hydroxy-butyrate had no effect on metastasis formation. \* $p < 0.01$ , PBS alone versus L-lactate (Student's t-test and ANOVA); \* $p < 0.05$ , PBS alone versus L-lactate (Mann-Whitney test).  $N = 20$  lung lobes counted for each group (B) Images of Lung Metastases. Representative examples of lung metastasis in PBS-alone controls and L-lactate-treated animals are shown. Note that the metastatic foci formed in L-lactate treated animals are more numerous, and are also larger in size.

where X is the width and Y is the length, was used in order to estimate tumor volume. The systemic administration of L-Lactate (500 mg/kg/mouse) and 3-hydroxy-butyrate (500 mg/kg/mouse)

was performed by daily intra-peritoneal (i.p.) injections, over a period of 3 weeks. Vehicle alone (PBS) was injected in control mice.

**Quantitation of tumor angiogenesis.** To quantify neo-vascularization, we performed CD31 immuno-histochemistry on frozen tumor sections, as previously described. Briefly, frozen tissue sections (6  $\mu\text{m}$ ) were fixed with acetone at  $-20^{\circ}\text{C}$  for 5 min and air dried. After blocking, the sections were incubated overnight at  $4^{\circ}\text{C}$  with a rat anti-mouse CD31 antibody at a dilution of 1:200, followed by a biotinylated rabbit anti-rat IgG (1:200) antibody and streptavidin-HRP. Immuno-reactivity was revealed with 3,3'-diaminobenzidine. Micro-vessel density was determined by counting CD31-positive vessels in six different fields for each tumor and average counts were recorded. Images were captured using a 20x objective lens and an ocular grid (0.25  $\text{mm}^2$  per field X6 fields) for a total of 1.5  $\text{mm}^2$ .

**Experimental metastasis (lung colonization assay).** For the metastasis study, tumor cells [MDA-MB-231 (GFP<sup>+</sup>) ( $5 \times 10^5$  cells)] re-suspended in 100  $\mu\text{l}$  of sterile PBS were injected via the tail vein of athymic nude mice and divided in three groups. Individual treatments, starting the same day of cell injection, with L-lactate (500 mg/kg/mouse), 3-hydroxy-butyrate (500 mg/kg/mouse) and PBS-alone as a control, were performed. After seven weeks of every-other-day intra-peritoneal injections, the lungs were removed and insufflated with 15% India Ink dye, washed in water and bleached in Fekete's solution (70% ethanol, 3.7% paraformaldehyde, 0.75 M glacial acetic acid). Surface lung colonies were counted in a blinded manner, under low power, using a Nikon (Tokyo, Japan) SMZ-1500 stereo-microscope. p-values were determined by applying Mann-Whitney statistical analysis, which does not assume a Gaussian distribution (non-parametric test).

**Cell migration assay.** The effects of L-lactate and 3-hydroxy-butyrate on the migratory potential of MDA-MB-231 cells was measured in vitro using a modified Boyden chamber assay. Briefly, MDA-MB-231 cells in 0.5 ml of serum-free Dulbecco's modified Eagle's medium were added to the wells of 8  $\mu\text{m}$  pore uncoated membrane of modified Boyden chambers. The lower chambers contained 10% fetal bovine serum in Dulbecco's modified Eagle's medium to serve as a chemo-attractant. Cells were incubated at  $37^{\circ}\text{C}$  and allowed to migrate throughout the course of 6 hours. Cells were removed from the upper surface of the membrane by scrubbing with cotton swabs. Chambers were stained in 0.5% crystal violet diluted in 100% methanol for 30 minutes, rinsed in water and examined under a bright-field microscope. Values for migration were obtained by counting five fields per membrane (X20 objective) and represent the average of three independent experiments. The metabolites L-lactate and 3-hydroxy-butyrate were individually placed in the lower chambers, at the concentration of 10 mM.

**Statistical analysis of animal studies and cell migration.** In general, statistical significance was examined using the Student's t-test. Values of  $p \leq 0.05$  were considered significant. Values were expressed as means  $\pm$  SEM.

**Gene set enrichment analysis.** Using raw transcriptional profiles,<sup>14</sup> we first composed a list of genes that are upregulated

**Table 1.** Breast cancer epithelial cells show a transcriptional shift towards oxidative mitochondrial metabolism, relative to adjacent stromal tissue

Gene set	Description	p-value
<b>Oxidative Phosphorylation</b>		
HSA00190_OXIDATIVE_PHOSPHORYLATION	Genes involved in oxidative phosphorylation	Less than 1.00E-16
MOOTHA_VOXPPOS	Oxidative Phosphorylation	Less than 1.00E-16
ELECTRON_TRANSPORT_CHAIN	Genes involved in electron transport	Less than 1.00E-16
OXIDATIVE_PHOSPHORYLATION	OXIDATIVE_PHOSPHORYLATION	3.81E-14
UBIQUINONE_BIOSYNTHESIS	UBIQUINONE_BIOSYNTHESIS	1.55E-06
<b>Mitochondrial Genes</b>		
MITOCHONDRION	Genes annotated by the GO term GO:0005739.	Less than 1.00E-16
A semiautonomous, self replicating organelle that occurs in varying numbers, shapes and sizes in the cytoplasm of virtually all eukaryotic cells. It is notably the site of tissue respiration.		
HUMAN_MITODB_6_2002	Mitochondrial genes	Less than 1.00E-16
MITOCHONDRIA	Mitochondrial genes	Less than 1.00E-16
MITOCHONDRIAL_PART	Genes annotated by the GO term GO:0044429.	2.22E-16
Any constituent part of a mitochondrion, a semiautonomous, self replicating organelle that occurs in varying numbers, shapes and sizes in the cytoplasm of virtually all eukaryotic cells. It is notably the site of tissue respiration.		
MITOCHONDRIAL_MEMBRANE	Genes annotated by the GO term GO:0031966.	3.77E-15
Either of the lipid bilayers that surround the mitochondrion and form the mitochondrial envelope.		
MITOCHONDRIAL_ENVELOPE	Genes annotated by the GO term GO:0005740.	1.17E-14
The double lipid bilayer enclosing the mitochondrion and separating its contents from the cell cytoplasm; includes the intermembrane space.		
MITOCHONDRIAL_INNER_MEMBRANE	Genes annotated by the GO term GO:0005743.	2.01E-13
The inner, i.e., lumen-facing, lipid bilayer of the mitochondrial envelope. It is highly folded to form cristae.		
MITOCHONDRIAL_MEMBRANE_PART	Genes annotated by the GO term GO:0044455.	1.53E-12
Any constituent part of the mitochondrial membrane, either of the lipid bilayers that surround the mitochondrion and form the mitochondrial envelope.		
MITOCHONDRIAL_RESPIRATORY_CHAIN	Genes annotated by the GO term GO:0005746.	4.42E-07
The protein complexes that form the mitochondrial electron transport system (the respiratory chain). Complexes I, III and IV can transport protons if embedded in an oriented membrane, such as an intact mitochondrial inner membrane.		
MITOCHONDRIAL_RESPIRATORY_CHAIN_COMPLEX_I	Genes annotated by the GO term GO:0005747.	2.09E-05
A part of the respiratory chain located in the mitochondrion. It contains about 25 different polypeptide subunits, including NADH dehydrogenase (ubiquinone), flavin mononucleotide and several different iron-sulfur clusters containing non-heme iron. The iron undergoes oxidation-reduction between Fe(II) and Fe(III), and catalyzes proton translocation linked to the oxidation of NADH by ubiquinone.		
NADH_DEHYDROGENASE_COMPLEX	Genes annotated by the GO term GO:0030964.	2.09E-05
An integral membrane complex that possesses NADH oxidoreductase activity. The complex is one of the components of the electron transport chain. It catalyses the transfer of a pair of electrons from NADH to a quinone.		
RESPIRATORY_CHAIN_COMPLEX_I	Genes annotated by the GO term GO:0045271.	2.09E-05
Respiratory chain complex I is an enzyme of the respiratory chain. It consists of at least 34 polypeptide chains and is L-shaped, with a horizontal arm lying in the membrane and a vertical arm that projects into the matrix. The electrons of NADH enter the chain at this complex.		
<b>TCA/Citric Acid Cycle</b>		
TCA	Tricarboxylic acid related genes	6.10E-06
CITRATE_CYCLE_TCA_CYCLE	CITRATE_CYCLE_TCA_CYCLE	1.35E-05
KREBS_TCA_CYCLE	KREBS_TCA_CYCLE	1.99E-05
HSA00620_PYRUVATE_METABOLISM	Genes involved in pyruvate metabolism	3.32E-05
HSA00020_CITRATE_CYCLE	Genes involved in citrate cycle (TCA cycle)	3.82E-07
<b>Biosynthesis and Energy</b>		
CELLULAR_BIOSYNTHETIC_PROCESS	Genes annotated by the GO term GO:0044249.	3.56E-13
The chemical reactions and pathways resulting in the formation of substances, carried out by individual cells.		
BIOSYNTHETIC_PROCESS	Genes annotated by the GO term GO:0009058.	4.74E-11
The energy-requiring part of metabolism in which simpler substances are transformed into more complex ones, as in growth and other biosynthetic processes.		

**Table 1.** Breast cancer epithelial cells show a transcriptional shift towards oxidative mitochondrial metabolism, relative to adjacent stromal tissue

Gene set	Description	p-value
MACROMOLECULE_BIOSYNTHETIC_PROCESS	Genes annotated by the GO term GO:0009059.	2.38E-10
The chemical reactions and pathways resulting in the formation of macromolecules, large molecules including proteins, nucleic acids and carbohydrates.		
ATP_SYNTHESIS	ATP_SYNTHESIS	1.64E-05
PURINE_METABOLISM	PURINE_METABOLISM	1.21E-06
PYRIMIDINE_METABOLISM	PYRIMIDINE_METABOLISM	6.39E-05
<b>Nutrient Starvation</b>		
PENG_LEUCINE_DN	Genes downregulated in response to leucine starvation	Less than 1.00E-16
PENG_GLUTAMINE_DN	Genes downregulated in response to glutamine starvation	Less than 1.00E-16
PENG_GLUCOSE_DN	Genes downregulated in response to glucose starvation	2.09E-08
<b>Alzheimer's Disease and Aging</b>		
ALZHEIMERS_DISEASE_DN	Downregulated in correlation with overt Alzheimer's Disease, in the CA1 region of the hippocampus	Less than 1.00E-16
ALZHEIMERS_INCIPIENT_DN	Downregulated in correlation with incipient Alzheimer's Disease, in the CA1 region of the hippocampus	3.05E-10
AGED_RHESUS_DN	Downregulated in the vastus lateralis muscle of aged vs. young adult rhesus monkeys	3.30E-09
AGED_MOUSE_CORTEX_DN	Downregulated in the cerebral cortex of aged (22 months) BALB/c mice, compared to young (2 months) controls	2.78E-06
OLD_FIBRO_DN	Downregulated in fibroblasts from old individuals, compared to young	2.42E-05
<b>Hypoxia</b>		
MANALO_HYPOXIA_DN	Genes downregulated in human pulmonary endothelial cells under hypoxic conditions or after exposure to AdCA5, an adenovirus carrying constitutively active hypoxia-inducible factor 1 (HIF-1alpha).	1.38E-06

in cancer epithelial vs. stromal cells for  $N = 28$  breast cancer patients. For each gene, we computed its differential expression in epithelial vs. stromal cells (normalized by the standard deviation) and its p-value, using a one-sided t-test. This list of upregulated genes was then tested for enrichment in gene sets contained in the latest release of Molecular Signatures Database (MSigDB v2.5, April 2008,<sup>53</sup>). MSigDB is a database of gene sets:

- collected from various sources, such as online pathway databases, publications and knowledge of domain experts,
- comprising genes that share a conserved cis-regulatory motif across the human, mouse, rat and dog genomes,
- identified as co-regulated gene clusters by mining large collections of cancer-oriented microarray data and
- annotated by a common Gene Ontology (GO) term.

The enrichment analysis consisted of computing p-values for the intersections between a gene list of interest  $X$  and each gene set  $Y$  in MSigDB. First, we computed the overlap between  $X$  and  $Y$ . Then, we computed the probability (p-value) that the observed overlap between sets  $X$  and  $Y$  is less than or equal to the overlap between set  $X$  and a randomly-chosen set of size equal to the size of set  $Y$ . This probability was calculated by applying the cumulative density function of the hypergeometric distribution on the size of set  $X$ , the size of set  $Y$ , the observed overlap between  $X$  and  $Y$  and the total number of available genes. In order to account for multiple hypothesis testing, we used randomly selected gene lists of the same size as the list under consideration to estimate the false discovery rate at a given p-value threshold. The final

list of significant MSigDB gene sets was determined by setting a p-value threshold which ensures that the false discovery rate does not exceed 5%. Additionally, we tested several gene lists each one consisting of the  $n$ -most upregulated genes for different values of  $n$  and found that the number of significant MSigDB gene sets maximized for  $n = 3,000$  at a 5% false discovery rate. Therefore, our final results are based on the top 3,000 upregulated genes.

#### Acknowledgements

M.P.L. and his laboratory were supported by grants from the NIH/NCI (R01-CA-080250; R01-CA-098779; R01-CA-120876; R01-AR-055660) and the Susan G. Komen Breast Cancer Foundation. F.S. was supported by grants from the W.W. Smith Charitable Trust, the Breast Cancer Alliance (BCA) and a Research Scholar Grant from the American Cancer Society (ACS). P.G.F. was supported by a grant from the W.W. Smith Charitable Trust and a Career Catalyst Award from the Susan G. Komen Breast Cancer Foundation. R.G.P. was supported by grants from the NIH/NCI (R01-CA-70896, R01-CA-75503, R01-CA-86072 and R01-CA-107382) and the Dr. Ralph and Marian C. Falk Medical Research Trust. The Kimmel Cancer Center was supported by the NIH/NCI Cancer Center Core grant P30-CA-56036 (to R.G.P.). Funds were also contributed by the Margaret Q. Landenberger Research Foundation (to M.P.L.). This project is funded, in part, under a grant with the Pennsylvania Department of Health (to M.P.L.). The Department specifically disclaims responsibility for any analyses,



interpretations or conclusions. This work was also supported, in part, by a Centre grant in Manchester from Breakthrough Breast Cancer in the U.K. (to A.H.) and an Advanced ERC Grant from the European Research Council.

## Note

Supplementary materials can be found at:

[www.landesbioscience.com/supplement/BonuccelliCC9-17-sup.xls](http://www.landesbioscience.com/supplement/BonuccelliCC9-17-sup.xls)

## References

- Witkiewicz AK, Dasgupta A, Sotgia F, Mercier I, Pestell RG, Sabel M, et al. An absence of stromal caveolin-1 expression predicts early tumor recurrence and poor clinical outcome in human breast cancers. *Am J Pathol* 2009; 174:2023-34.
- Witkiewicz AK, Dasgupta A, Sammons S, Er O, Potoczek MB, Guiles F, et al. Loss of stromal caveolin-1 expression predicts poor clinical outcome in triple negative and basal-like breast cancers. *Cancer Biol Ther* 2010; 10:135-143.
- Sloan EK, Ciocca D, Pouliot N, Natoli A, Restall C, Henderson M, et al. Stromal cell expression of caveolin-1 predicts outcome in breast cancer. *Am J Pathol* 2009; 174:2035-43.
- Witkiewicz AK, Dasgupta A, Nguyen KH, Liu C, Kovatich AJ, Schwartz GF, et al. Stromal caveolin-1 levels predict early DCIS progression to invasive breast cancer. *Cancer Biol Ther* 2009; 8:1167-75.
- Di Vizio D, Morello M, Sotgia F, Pestell RG, Freeman MR, Lisanti MP. An absence of stromal caveolin-1 is associated with advanced prostate cancer, metastatic disease and epithelial Akt activation. *Cell Cycle* 2009; 8:2420-4.
- Razani B, Engelman JA, Wang XB, Schubert W, Zhang XL, Marks CB, et al. Caveolin-1 null mice are viable but show evidence of hyperproliferative and vascular abnormalities. *J Biol Chem* 2001; 276:38121-38.
- Pavrides S, Whitaker-Menezes D, Castello-Cros R, Flomenberg N, Witkiewicz AK, Frank PG, et al. The reverse Warburg effect: Aerobic glycolysis in cancer associated fibroblasts and the tumor stroma. *Cell Cycle* 2009; 8:3984-4001.
- Pavrides S, Tsirogas A, Vera I, Flomenberg N, Frank PG, Casimiro MC, et al. Loss of stromal caveolin-1 leads to oxidative stress, mimics hypoxia and drives inflammation in the tumor microenvironment, conferring the "Reverse Warburg Effect": A transcriptional informatics analysis with validation. *Cell Cycle* 2010; 9:2201-2219.
- Bonuccelli G, Whitaker-Menezes D, Castello-Cros R, Pavrides S, Pestell RG, Fatatis A, et al. The Reverse Warburg Effect: Glycolysis inhibitors prevent the tumor promoting effects of caveolin-1 deficient cancer associated fibroblasts. *Cell Cycle* 2010; 9:1960-1971.
- Pavrides S, Tsirogas A, Vera I, Flomenberg N, Frank PG, Casimiro MC, et al. Transcriptional evidence for the "Reverse Warburg Effect" in human breast cancer tumor stroma and metastasis: similarities with oxidative stress, inflammation, Alzheimer's disease and "Neuron-Glia Metabolic Coupling". *Aging (Albany NY)* 2010; 2:185-99.
- Martinez-Outschoorn UE, Balliet R, Rivadeneira D, Chiavarina B, Pavrides S, Wang C, et al. Oxidative stress in cancer associated fibroblasts drives tumor-stroma co-evolution: A new paradigm for understanding tumor metabolism, the field effect and genomic instability in cancer cells. *Cell Cycle* 2010; 9:3256-3276.
- Martinez-Outschoorn UE, Pavrides S, Whitaker-Menezes D, Daumer KM, Millman JN, Chiavarina B, et al. Tumor cells induce the cancer associated fibroblast phenotype via caveolin-1 degradation: Implications for breast cancer and DCIS therapy with autophagy inhibitors. *Cell Cycle* 2010; 9:2423-2433.
- Pavrides S, Tsirogas A, Migneco G, Whitaker-Menezes D, Chiavarina B, Flomenberg N, et al. The autophagic tumor stroma model of cancer: Role of oxidative stress and ketone production in fueling tumor cell metabolism. *Cell Cycle* 2010; 9: 3485-505.
- Casey T, Bond J, Tighe S, Hunter T, Lintault L, Patel O, et al. Molecular signatures suggest a major role for stromal cells in development of invasive breast cancer. *Breast Cancer Res Treat* 2009; 114:47-62.
- Cahill GF Jr, Veech RL. Ketoacids? Good medicine? *Trans Am Clin Climatol Assoc* 2003; 114:149-61.
- Veech RL. The therapeutic implications of ketone bodies: the effects of ketone bodies in pathological conditions: ketosis, ketogenic diet, redox states, insulin resistance and mitochondrial metabolism. *Prostaglandins Leukot Essent Fatty Acids* 2004; 70:309-19.
- Veech RL, Chance B, Kashiwaya Y, Lardy HA, Cahill GF Jr. Ketone bodies, potential therapeutic uses. *IUBMB Life* 2001; 51:241-7.
- Zou Z, Sasaguri S, Rajesh KG, Suzuki R. dl-3-Hydroxybutyrate administration prevents myocardial damage after coronary occlusion in rat hearts. *Am J Physiol Heart Circ Physiol* 2002; 283:1968-74.
- Puchowicz MA, Zechel JL, Valerio J, Emancipator DS, Xu K, Pundik S, et al. Neuroprotection in diet-induced ketotic rat brain after focal ischemia. *J Cereb Blood Flow Metab* 2008; 28:1907-16.
- Nicolucci A. Epidemiological aspects of neoplasms in diabetes. *Acta Diabetol* 2010; 47:87-95.
- Sauer LA, Dauchy RT. Stimulation of tumor growth in adult rats in vivo during acute streptozotocin-induced diabetes. *Cancer Res* 1987; 47:1756-61.
- Goodstein ML, Richtsmeier WJ, Sauer LA. The effect of an acute fast on human head and neck carcinoma xenograft. Growth effects on an 'isolated tumor vascular pedicle' in the nude rat. *Arch Otolaryngol Head Neck Surg* 1993; 119:897-902.
- Koukourakis MI, Kontomanolis E, Giatromanolaki A, Sivridis E, Liberis V. Serum and tissue LDH levels in patients with breast/gynaecological cancer and benign diseases. *Gynecol Obstet Invest* 2009; 67:162-8.
- Ryberg M, Nielsen D, Osterlind K, Andersen PK, Skovsgaard T, Dombrowsky P. Predictors of central nervous system metastasis in patients with metastatic breast cancer. A competing risk analysis of 579 patients treated with epirubicin-based chemotherapy. *Breast Cancer Res Treat* 2005; 91:217-25.
- Nisman B, Barak V, Hubert A, Kaduri L, Lyass O, Baras M, et al. Prognostic factors for survival in metastatic breast cancer during first-line paclitaxel chemotherapy. *Anticancer Res* 2003; 23:1939-42.
- Ryberg M, Nielsen D, Osterlind K, Skovsgaard T, Dombrowsky P. Prognostic factors and long-term survival in 585 patients with metastatic breast cancer treated with epirubicin-based chemotherapy. *Ann Oncol* 2001; 12:81-7.
- Vigano A, Bruera E, Jhangri GS, Newman SC, Fields AL, Suarez-Almazor ME. Clinical survival predictors in patients with advanced cancer. *Arch Intern Med* 2000; 160:861-8.
- Kher A, Moghe G, Deshpande A. Significance of serum ferritin and lactate dehydrogenase in benign and malignant disease of breast. *Indian J Pathol Microbiol* 1997; 40:321-6.
- Khan N, Tyagi SP, Salahuddin A. Diagnostic and prognostic significance of serum cholinesterase and lactate dehydrogenase in breast cancer. *Indian J Pathol Microbiol* 1991; 34:126-30.
- Yeshowardhana, Gupta MM, Bansal G, Goyal S, Singh VS, Jain S, Sangita Jain K. Serum glycolytic enzymes in breast carcinoma. *Tumori* 1986; 72:35-41.
- Malhotra P, Sidhu LS, Singh SP. Serum lactate dehydrogenase level in various malignancies. *Neoplasma* 1986; 33:641-7.
- Lee YT. Biochemical and hematological tests in patients with breast carcinoma: correlations with extent of disease, sites of relapse and prognosis. *J Surg Oncol* 1985; 29:242-8.
- Al-Mondhary H. Disseminated intravascular coagulation: experience in a major cancer center. *Thromb Diath Haemorrh* 1975; 34:181-93.
- Colombo GM, Del Vecchio LR, Sacco T, Cicchinelli M. Fatal lactic acidosis due to widespread diffusion of melanoma. *Minerva Med* 2006; 97:295.
- Deeren D, Verbeken E, Vanderschueren S, Wilmer A, Bobbaers H, Meersseman W. Cancer presenting as fatal pulmonary tumour embolism. *Acta Clin Belg* 2006; 61:30-4.
- Cheng JC, Esparza SD, Knez VM, Sakamoto KM, Moore TB. Severe lactic acidosis in a 14-year-old female with metastatic undifferentiated carcinoma of unknown primary. *J Pediatr Hematol Oncol* 2004; 26:780-2.
- Chau WK, Yang CF, Chou YH, Ho CH. Aggressive undifferentiated carcinoma of unknown primary site complicated by lactic acidosis after bleeding: a case report. *Jpn J Clin Oncol* 2002; 32:210-4.
- Wall BM, Mansour N, Cooke CR. Acute fulminant lactic acidosis complicating metastatic cholangiocarcinoma. *Am J Med Sci* 2000; 319:126-9.
- Evans TR, Stein RC, Ford HT, Gazet JC, Chamberlain GV, Coombes RC. Lactic acidosis. A presentation of metastatic breast cancer arising in pregnancy. *Cancer* 1992; 69:453-6.
- Warner E. Type B lactic acidosis and metastatic breast cancer. *Breast Cancer Res Treat* 1992; 24:75-9.
- Odeh M, Bassan H. The role of malignancy in lactic acidosis and shock. *Postgrad Med J* 1989; 65:801.
- Thomas CR Jr, Dodhia N. Common emergencies in cancer medicine: metabolic syndromes. *J Natl Med Assoc* 1991; 83:809-18.
- Sculier JP, Nicaise C, Klastersky J. Lactic acidosis: a metabolic complication of extensive metastatic cancer. *Eur J Cancer Clin Oncol* 1983; 19:597-601.
- Sheriff DS. Lactic acidosis and small cell carcinoma of the lung. *Postgrad Med J* 1986; 62:297-8.
- Raju RN, Kardinal CG. Lactic acidosis in lung cancer. *South Med J* 1983; 76:397-8.
- Stacpoole PW, Lichtenstein MJ, Polk JR, Greco FA. Lactic acidosis associated with metastatic osteogenic sarcoma. *South Med J* 1981; 74:868-70.
- Varanasi UR, Carr B, Simpson DP. Lactic acidosis associated with metastatic breast carcinoma. *Cancer Treat Rep* 1980; 64:1283-5.
- Wesbey G. Lactic acidosis in oat cell carcinoma with extensive hepatic metastases. *Arch Intern Med* 1981; 141:816-7.
- Kachel RG. Metastatic reticulum cell sarcoma and lactic acidosis. *Cancer* 1975; 36:2056-9.
- Belt JA, Thomas JA, Buchsbaum RN, Racker E. Inhibition of lactate transport and glycolysis in Ehrlich ascites tumor cells by bioflavonoids. *Biochemistry* 1979; 18:3506-11.
- Hu Q, Noor M, Wong YF, Hylands PJ, Simmonds MS, Xu Q, et al. In vitro anti-fibrotic activities of herbal compounds and herbs. *Nephrol Dial Transplant* 2009; 24:3033-41.
- Phan TT, Lim JJ, Chan SY, Tan EK, Lee ST, Longaker MT. Suppression of transforming growth factor beta/smud signaling in keloid-derived fibroblasts by quercetin: implications for the treatment of excessive scars. *J Trauma* 2004; 57:1032-7.
- Subramanian A, Tamayo P, Mootha VK, Mukherjee S, Ebert BL, Gillette MA, et al. Gene set enrichment analysis: a knowledge-based approach for interpreting genome-wide expression profiles. *Proc Natl Acad Sci USA* 2005; 102:15545-50.